



HAL
open science

Glutamate decarboxylase67 is expressed in hippocampal mossy fibers of temporal lobe epilepsy patients

Günther Sperk1

► **To cite this version:**

Günther Sperk1. Glutamate decarboxylase67 is expressed in hippocampal mossy fibers of temporal lobe epilepsy patients. *Hippocampus*, 2011, 22 (3), pp.590. 10.1002/hipo.20923 . hal-00686077

HAL Id: hal-00686077

<https://hal.science/hal-00686077>

Submitted on 7 Apr 2012

HAL is a multi-disciplinary open access archive for the deposit and dissemination of scientific research documents, whether they are published or not. The documents may come from teaching and research institutions in France or abroad, or from public or private research centers.

L'archive ouverte pluridisciplinaire **HAL**, est destinée au dépôt et à la diffusion de documents scientifiques de niveau recherche, publiés ou non, émanant des établissements d'enseignement et de recherche français ou étrangers, des laboratoires publics ou privés.



Glutamate decarboxylase67 is expressed in hippocampal mossy fibers of temporal lobe epilepsy patients

Journal:	<i>Hippocampus</i>
Manuscript ID:	HIPO-10-173.R2
Wiley - Manuscript type:	Research Article
Keywords:	GABA, GAD67, VGAT, inverse GABA transport, plasticity

SCHOLARONE™
Manuscripts

Review

1
2 Re-revised Manuscript
3

4 **Glutamate decarboxylase67 is expressed in hippocampal mossy fibers of**
5 **temporal lobe epilepsy patients**
6
7

8
9
10
11 **Günther Sperk¹, Anna Wieselthaler-Hözl¹, Susanne Pirker^{1,2}, Ramon Tasan¹, Sarah S.**
12 **Strasser¹, Meinrad Drexel¹, Christian Pifl³, Julian Marschalek⁴, Martin Ortler⁵, Eugen**
13 **Trinka⁶, Katja Haitmalr-Wietzorrek¹, Philippe Ciofi⁷, Martha Feucht⁸, Christoph**
14 **Baumgartner², Thomas Czech⁴**
15
16
17

18
19 ¹Department of Pharmacology, Medical University Innsbruck, Austria

20 ²Karl Landsteiner Institute for Clinical Epilepsy Research and Cognitive Neurology, General
21 Hospital Hietzing with Neurological Center Rosenhügel, Vienna, Austria
22

23 ³Center for Brain Research, Medical University of Vienna, Vienna, Austria

24 ⁴Clinical Department of Neurosurgery, Medical University of Vienna, Vienna, Austria

25 ⁵Clinical Department of Neurosurgery, Medical University Innsbruck, Innsbruck,
26 Austria
27

28 ⁶Clinical Department of Neurology, Medical University Innsbruck, Austria

29 ⁷Institut National de la Santé et de la Recherche Médicale (INSERM), Neurocentre Magendie-
30 Unité 862, Bordeaux, France
31

32 ⁸University Clinics for Children and Adolescents, Medical University Vienna, Vienna, Austria
33
34
35

36
37
38
39
40 Running title: GAD67 in hippocampal mossy fibers
41

42
43 Correspondence to:

44 Dr. Günther Sperk

45 Department of Pharmacology

46 Peter-Mayr-Str. 1a

47 A-6020 Innsbruck

48 Austria

49 Tel: +43-512-9003-71210

50 Fax: +43-512-9003-73200

51 E-mail: guenther.sperk@i-med.ac.at
52
53
54
55

56 **KEY WORDS: GABA, GAD67, VGAT, inverse GABA transport, plasticity**
57
58

59 Grant sponsor: Austrian Science Foundation, grant numbers: P 19 464, SFB 35-12; grant
60 sponsor: European Union Grant FP6 EPICURE, grant number: LSH-CT-2006-037315.

ABSTRACT

1
2
3
4
5 Recently, expression of glutamate decarboxylase-67 (GAD67), a key enzyme of GABA
6 synthesis, was detected in the otherwise glutamatergic mossy fibers of the rat hippocampus.
7
8 Synthesis of the enzyme was markedly enhanced after experimentally induced status
9 epilepticus. Here, we investigated the expression of GAD67 protein and mRNA in 44
10 hippocampal specimens from patients with mesial temporal lobe epilepsy (TLE) using double
11 immunofluorescence histochemistry, immunoblotting and *in situ* hybridization. Both in
12 specimens with (n = 37) and without (n = 7) hippocampal sclerosis, GAD67 was highly co-
13 expressed with dynorphin in terminal areas of mossy fibers, including the dentate hilus and the
14 stratum lucidum of sector CA3. In the cases with Ammon's horn sclerosis, also the inner
15 molecular layer of the dentate gyrus contained strong staining for GAD67 immunoreactivity,
16 indicating labeling of mossy fiber terminals that specifically sprout into this area. Double
17 immunofluorescence revealed the co-localization of GAD67 immunoreactivity with the mossy
18 fiber marker dynorphin. **The extent of co-labelling correlated with the number of seizures**
19 **experienced by the patients.** Furthermore, GAD67 mRNA was found in granule cells of the
20 dentate gyrus. Levels, both of GAD67 mRNA and of GAD67 immunoreactivity were similar in
21 sclerotic and non-sclerotic specimens and appeared to be increased compared to post mortem
22 controls. Provided that the strong expression of GAD67 results in synthesis of GABA in
23 hippocampal mossy fibers this may represent a self-protecting mechanism in TLE. In addition
24 GAD67 expression also may result in conversion of excessive intracellular glutamate to non-
25 toxic GABA within mossy fiber terminals.
26
27
28
29
30
31
32
33
34
35
36
37
38
39
40
41
42
43
44
45
46
47
48
49
50
51
52
53
54
55
56
57
58
59
60

INTRODUCTION

Mesial temporal lobe epilepsies (TLE) are among the most severe forms of focal epilepsies. Up to 80% of TLE patients do not adequately respond to therapies based on currently available antiepileptic drugs. Epilepsy surgery removing the epileptogenic tissue in the mesial temporal lobe offers a valuable treatment option for these patients with a seizure-free outcome or marked reduction of seizure frequency of more than 70-90% (Wiebe et al., 2001). The examination of tissue obtained from TLE patients at surgery and study of animal models of TLE have revealed widespread molecular, morphologic, and neurophysiological rearrangement of the epileptic hippocampus (Houser and Esclapez, 1994; Mikkonen et al., 1998; Mathern et al., 1999; Pirker et al., 2001). In particular, granule cells of the dentate gyrus display remarkable plasticity, which is accompanied by altered expression of numerous functionally relevant peptides and proteins, including growth factors, neurotransmitter receptors, and ion channels. The axons of granule cells, the mossy fibers, sprout and aberrantly target the inner molecular layer of the dentate gyrus where they appear to substitute for innervation by associational/commissural fibers from hilar mossy cells, which degenerate in the epileptic hippocampus (Sutula et al., 1989).

Granule cells of the dentate gyrus give rise to a fiber bundle, the so-called mossy fibers, which innervate CA3 pyramidal neurons. They are excitatory and use glutamate as their principal neurotransmitter (Bramham et al., 1990). Mossy fiber terminals are rich in dense core vesicles that also contain neuropeptides, including dynorphin and chromogranins (Pirker et al., 2001). Using electron microscopy, Sandler and Smith (1991) demonstrated the presence of GABA in close vicinity to the synaptic vesicles of mossy fibers in the monkey hippocampus. Since then, several groups have reported that mossy fibers in rats and monkeys also express glutamate decarboxylase-67 (GAD67), which catalyzes the synthesis of GABA from glutamate, and that levels of GAD67 mRNA and protein are enhanced in granule cells/mossy fibers after sustained epileptic seizures in rats (Schwarzer and Sperk, 1995; Sloviter et al., 1996; Sperk et al., 2003). Subsequent studies indicated that stimulation of granule cells causes release of GABA from mossy fiber terminals, activating postsynaptic GABA_A receptors and leading to hyperpolarization of CA3 neurons (Gutierrez and Heinemann, 2001; Walker et al., 2001). **The data suggest that the synthesis and release of GABA from mossy fibers could be an endogenous mechanism for seizure termination or to convert excess glutamate into GABA (Sperk et al., 2003).**

In the present study, we addressed the question of whether GAD67 is also expressed in mossy fibers of the human epileptic hippocampus. Using specimens from patients with TLE obtained at surgery and immunohistochemically, we demonstrate co-expression of GAD67 with the mossy fiber marker dynorphin in terminal areas of mossy fibers (Houser et al., 1990), including the dentate hilus, the stratum lucidum, and the inner molecular layer, which becomes innervated by sprouted mossy fibers in Ammon's horn sclerosis.

PATIENTS AND METHODS

Patients

This study conforms to The Code of Ethics of the World Medical Association (Declaration of Helsinki). Approval for this study was obtained from the Institutional Boards of the Medical Universities Vienna and Innsbruck, Austria and informed consent was obtained from all patients providing specimens. Specimens were obtained at surgery from 44 patients (24 females and 20 males) with chronic pharmaco-resistant TLE who had undergone unilateral selective amygdalo-hippocampectomy or anteromedial temporal lobe resection. Clinical data are shown in Table 1. Thirty seven specimens had moderate to severe, seven cases no or only minimal Ammon's horn sclerosis (termed non-sclerotic). The age of patients at surgery ranged from 9 to 65 years (mean \pm SEM, 35 ± 1.9 years). The time between onset of epilepsy and surgery ranged from 3 to 51 years. The decision for surgery was based on converging evidence from EEG recordings during prolonged video-EEG monitoring with scalp and sphenoidal electrodes, ictal perfusion SPECT (single photon emission computed tomography) using [123 I]HMPAO (hexamethyl propylene amine oxime), high-resolution magnetic resonance imaging and formal neuropsychological tests indicating a unilateral and mesial temporal lobe onset of seizures.

Post-mortem tissue from non-epileptic patients

Hippocampal tissue was obtained at routine autopsy from 11 patients (2 females, 9 males) with no known history of any neurological or psychiatric disease (Table 2). The time from death to snap freezing respectively paraformaldehyde (PFA) fixation (contralateral side) of brain specimens ranged from 8 to 16 h (11.6 ± 0.93 h). The mean age at death was 52.5 ± 5.6 years. Causes of death were pulmonary embolism, liver cirrhosis, cardiovascular arrest, leukemia, melanoma, and cancer of the pharynx, trachea, and breast.

Preparation and fixation of specimens

Hippocampal specimens were rinsed in 50 mM phosphate-buffered saline, pH 7.4 (PBS) at 4°C and sectioned perpendicularly to the hippocampal axis into 5-mm blocks. Those obtained from the hippocampal body (middle segment) were included in the study. Tissue blocks were either rapidly snap frozen for immunoblotting ($n = 8$ TLE specimens and 8 post mortem controls) or fixed with PFA for immunohistochemistry and *in situ* hybridization (44 TLE specimens and 11 post mortem controls). These were immediately immersed in 4% paraformaldehyde in PBS for 4 to 5 days followed by stepwise immersion in sucrose (concentrations ranging from 5–20%) over 2 days and then snap frozen (-70°C cold isopentane, 3 min). After allowing the isopentane to evaporate for 24 h at -70°C , tissue samples were sealed in vials and stored at -70°C . For immunohistochemistry, microtome sections (40 μm) were collected and kept for up to 2 weeks

1
2 in PBS containing 0.1% sodium azide at 5 °C to reduce endogenous peroxidase activity. For *in*
3 *situ* hybridization, 20 µm sections were cut, mounted on poly-L-lysine-coated slides and stored
4 at -20 °C.
5
6

7 8 **Immunohistochemistry** 9

10 Antibodies: GAD67-immunoreactivity (IR) was studied using a monoclonal mouse GAD67-
11 specific antibody (1:10,000; IgG2α, clone1G10.2; Chemicon, MAB5406). The antibody was
12 highly specific for GAD67 in immunoblots. A rabbit antiserum targeting dynorphin A (1-8)
13 (1:20,000) (Pirker et al., 2001; Pirker et al., 2009) was used to label mossy fibers. For labeling
14 terminals of GABA-ergic neurons, an affinity-purified rabbit antiserum against a fusion protein of
15 the N-terminal sequence of the vesicular GABA transporter (VGAT) with glutathione S-
16 transferase (1:1,000;) was applied (Chaudhry et al., 1998). For glutamate decarboxylase65
17 (GAD65) a commercially available rabbit antibody (1:5,000; AB 5082, Chemicon; Millipore,
18 Vienna, Austria) was used. For detection of neuronal nuclear protein (NeuN), a monoclonal
19 mouse antibody (1:5,000; MAB 377; Chemicon, Millipore, Vienna, Austria) was used.
20
21
22
23
24
25
26
27

28 Adjacent free-floating 40-µm sections were used for immunohistochemistry. Sections were pre-
29 treated with target retrieval solution (pH 6.0; Dako, Vienna, Austria, 70 °C, 20 min) and, after
30 washing in 50 mM Tris-buffered saline pH 7.2 (TBS) for 5 min, with 0.6% H₂O₂, 20%
31 methanol/TBS for 20 min to reduce endogenous peroxidase activity. They were then incubated
32 in 10% normal horse serum (for GAD67 and NeuN) or 10% normal goat serum (for dynorphin,
33 VGAT and GAD65; both VWR, Vienna, Austria) in TBS for 90 min and subsequently with the
34 primary antiserum at 4 °C for 48–72 hr. The sections were then processed by the Vectastain
35 ABC standard procedure using 1:200 dilutions of Vectastain PK4002 horse biotinylated anti-
36 mouse antibody for detecting the GAD67 and NeuN mouse antibodies, and Vectastain PK4001
37 goat biotinylated anti-rabbit antibody for detecting the rabbit VGAT and dynorphin antibodies
38 (Vector, Szabo-Scandic, Vienna, Austria). Incubations with the biotinylated secondary
39 antibodies and subsequent incubations with the ABC reagent (mixture of avidin-biotin-
40 horseradish peroxidase complex; 1:100) were done at room temperature for 60 min each. The
41 resulting complex was labeled by reacting the peroxidase with 0.05% 3,3'-diaminobenzidine
42 (Sigma, Munich, Germany) and 0.005% H₂O₂ in TBS for 4 min. Sections were mounted on
43 slides, air-dried, dehydrated, and cover-slipped. After each incubation step (except pre-
44 incubation with 10% normal horse serum), three 5 min washes with TBS were included. All
45 buffers and antibody dilutions, except those for washing after target retrieval solution and
46 peroxidase treatment, and the reaction with diaminobenzidine, contained 0.1% Triton X-100.
47 Normal horse or goat serum (10%) was included in all antibody-containing buffers. Sections not
48 exposed to the primary antibody were included as controls and did not show immunoreactive
49 elements.
50
51
52
53
54
55
56
57
58
59
60

Double immunofluorescence

Double immunofluorescence was performed on sections from six selected patients. Incubations were done using free-floating 40- μ m sections. After subjecting them to target retrieval treatment and peroxidase block, incubations were processed as described above using concomitant incubations with the monoclonal GAD67 antibody (dilution of 1:5,000), and with the rabbit dynorphin A (1-8) antibody (1:10,000) or the VGAT antiserum (1:1,000). For co-labeling of GAD67-IR and dynorphin-IR or GAD67 and VGAT, an Alexa 555-coupled goat anti-mouse antibody (IgG2 α ; 1:500; Molecular Probes; Eubio, Vienna, Austria) for detecting GAD67-IR and an Alexa AF488-coupled donkey anti-rabbit antibody (1:1,000; Molecular Probes; Eubio, Vienna, Austria) for detecting dynorphin and VGAT, respectively, were used as secondary antibodies. The sections were embedded in Vectashield (Vector Laboratories; Szabo-Scandic, Vienna, Austria) in 0.5% gelatin/0.05% chrome alum on uncoated slides. A Zeiss Axioplan-2 fluorescence microscope equipped with a CCD camera (AxioCam, Zeiss, Vienna) was used for recording images. These were analyzed and displayed using Openlab software (version 3.0.2; Improvision, Tübingen, Germany).

In situ hybridization

In situ hybridization was performed on 20- μ m sections from 36 TLE patients and 9 post mortem controls. An oligonucleotide complementary to bases 203-252 of human GAD67 mRNA (Bu et al., 1992), (GenBank accession number NM_000817.2: AGCTGCTTCCTCGTTCTCGCTAGTTCCTCTCGCACGCGAGCGCCAGGAG) was synthesized by Microsynth (Balgach, Switzerland). It was labeled with [³⁵S] α -thio-dATP (1,300 Ci/mmol; New England Nuclear, Boston, MA, USA) on the 3' end by reaction with terminal deoxynucleotidyl transferase (Roche, Mannheim, Germany), and *in situ* hybridization was performed as described previously (Furtinger et al., 2001). After washing stringently (four times in 50% formamide in 2 \times SSC; 42°C, 15 min), the sections were briefly rinsed in 1 \times SSC followed by water, dipped in 70% ethanol, dried, and exposed to BioMax MR films (Amersham Pharmacia Biotech, Buckinghamshire, UK) for 21 days. An excess of non-radioactive probe displaced the radioactive labeling and was used as control. The relative amount of GAD67-specific hybridization signal was determined over the granule cell layer by densitometric analysis of film autoradiograms using the ImageJ analysis system (written by Wayne Rasband at the U.S. National Institutes of Health and available from the Internet by anonymous FTP from zippy.nimh.nih.gov). Changes in hybridization signal intensity in TLE specimens were quantified by determining the percent difference in relative optical density (ROD) in control tissue sections relative to experimental tissue sections processed in parallel. Background values were determined in the adjacent white matter and subtracted from ROD values. Calibration and linearization of film autoradiograms were performed relative to ¹⁴C-labeled autoradiographic standards (microscales, New England Nuclear, Boston, MA, USA), which were exposed to each

1
2 film simultaneously with hybridized tissue sections.
3

4
5 **Neuronal cell counts.** After autoradiography the sections were Nissl-stained and cell counts
6 were performed in three different 250 × 100- μ m areas of the granule cell layer, and values were
7 averaged. An ocular grid (100 boxes of 2.5 × 2.5 μ m each) was used at 400 \times magnification.
8
9

10 11 **Neurodegeneration rating**

12 Neurodegeneration rating was performed independently by two blinded observers using Nissl-
13 stained sections adjacent to the sections used for immunohistochemistry and the following
14 rating scale (Davies et al., 1996): 0, no obvious neurodegeneration; 1, modest cell losses (up to
15 about 10%) of pyramidal neurons (primarily CA1) and/ or hilar interneurons; 2, minor but
16 obvious cell losses of hilar interneurons and CA1 and CA3 pyramidal cells; 3, significant cell
17 losses in the hilus of the dentate gyrus (only a few cells are visible), major parts of the CA1 and
18 CA3 sector of the Ammon's horn are affected; 4, clear-cut losses in dentate granule cells and
19 CA2 neurons in addition to severe damage of hilar interneurons and CA1 and CA3 pyramidal
20 neurons.
21
22
23
24
25
26
27
28
29

30 **Rating of granule cell dispersion**

31 Granule cell dispersion was rated as follows: 0, no obvious dispersion; 1, modest dispersion; 2,
32 more than 30% of the granule cell layer is broadened by approximately 50–100%; 3, more than
33 half of the granule cell layer is affected and its width is significantly increased (generally by
34 100% or more). At ratings 2 and 3, the density of the granule cell layer often loosens and
35 significant neurodegeneration can lead to segments of even reduced layer width. Double
36 granule cell layer can be seen in over 20% of cases (labeled D in Table 1).
37
38
39
40
41
42

43 **Evaluation of co-distribution of GAD67-IR and dynorphin-IR after conventional** 44 **immunohistochemistry**

45 The distribution of GAD67-IR, dynorphin-IR, and VGAT-IR was assessed in adjacent sections
46 processed by the avidin-biotin-peroxidase method. We assessed the extent of co-labeling in the
47 following terminal structures of mossy fibers: *i*) the hilus of the dentate gyrus (bundles of mossy
48 fibers; plaques presumably originating from degenerating mossy fibers); *ii*) the terminal area of
49 mossy fibers in the stratum lucidum (no or minor overlap with VGAT-IR); *iii*) the area of sprouted
50 mossy fiber terminals in the inner molecular layer.
51
52
53
54
55
56

57 A rating scale for the likelihood of co-distribution of GAD67-IR and dynorphin-IR was adapted.
58 Two independent observers rated the patterns of GAD67 and dynorphin co-labeling at all three
59 sites using a four-point rating scale: 0, co-labeling unlikely; 1, co-labeling possible; 2, co-
60

1
2 labeling likely; 3, co-labeling evident. Independent ratings were obtained for all three sites by
3
4 the two observers, and mean values were obtained from these data.
5
6

7 Immunoblotting

8 Cryotome sections (20 μm) of snap frozen, unfixed hippocampal specimens were obtained from
9 controls ($n = 8$) and sclerotic TLE patients ($n = 8$) and mounted on slides. For each specimen,
10 the area of the dentate gyrus was scraped off from six sections using a spatula and collected in
11 an Eppendorf vial. Tissues were homogenized in 10 mM HEPES pH 7.5, 1 mM EDTA, 1 mM
12 benzamidine, 0.3 mM phenylmethylsulfonyl fluoride, 100 mg/l bacitracin (all Sigma, Munich,
13 Germany) by mild sonication. Samples were centrifuged ($8,000 \times g$, 20 min, 4°C). Supernatants
14 were denatured (15 min, 65°C) in sample buffer (NP0007, Invitrogen, Lofer, Austria) under
15 reducing conditions (10% reducing agent NP0001; Invitrogen). Samples (5 μg protein) were run
16 on 4–12% NuPAGE Bis-Tris gels with a MOPS running buffer (NP0321, Invitrogen) and blotted
17 onto polyvinylidene difluoride (PVDF) membranes (SequiBlot, BioRad, Vienna, Austria),
18 according to the standard procedures of the manufacturers. Membranes were blocked (2 h,
19 room temperature) in 2.5% skim milk in TBS containing 0.1% Tween 20 (Merck, Darmstadt,
20 Germany) and then incubated with the primary GAD67 antibody (0.3 $\mu\text{g}/\text{ml}$; IgG2 α ,
21 clone1G10.2; Chemicon, MAB5406) in the same buffer at 4°C over night. Subsequently,
22 labeling with a mouse monoclonal neuron-specific enolase (NSE) antibody (ab8197, Abcam,
23 Cambridge, UK; 1:4,000, 1 hr at room temperature) was performed as an internal standard. In
24 both instances, a horseradish peroxidase-conjugated secondary antibody (rabbit anti-mouse
25 IgG, P260, Dako, Vienna, Austria; 1:4,000, 90 min) was applied in TBS-Tween 20. Pre-stained
26 size markers (See Blue Plus 2, LC 5925, Invitrogen, Lofer, Austria) were used for calibration.
27 Enhanced chemoluminescence was used for signal detection. Films were exposed for 5 s
28 (NSE) and 5 to 10 min (GAD67), respectively, and then digitized. The relative optical densities
29 (ROD) of bands corresponding to GAD67 and NSE were determined. Data are expressed as
30 ratios of GAD67 and NSE values.
31
32
33
34
35
36
37
38
39
40
41
42
43
44
45
46
47

48 Determination of GABA levels

49 Amino acid levels were determined in the dentate gyri of 10 sclerotic TLE patients and six post-
50 mortem controls. Hippocampal slices (40 μm) were cut in a microtome. The dentate gyri were
51 removed under a dissection microscope, transferred to an Eppendorf tube, weighed, and
52 frozen. The samples were then sonicated in 50 volumes of 0.1 M perchloric acid, centrifuged for
53 15 min at $13,000 \times g$ at 4°C , and the supernatants were frozen at -80°C until analysis. Samples
54 were thawed and diluted with H_2O (final dilution 1:2,000). Each sample (100 μl) was then mixed
55 with 50 μl OPA-reagent (25 mg o-phthalaldehyde dissolved in a mixture of 0.5 ml methanol, 25
56 μl mercaptoethanol, and 4.5 ml 0.4-M sodium borate, pH 11), and after a reaction time of 2 min,
57 20 μl was injected by an autosampler (AS950, Jasco). The HPLC system consisted of a RP-18
58
59
60

1 column (Chromolith-Performance RP-18e, 100 x 4.6mm, Merck) in a column-heater set a 25 °C
2 (BFO-04 f1, W.O. Electronics), and an aqueous mobile phase containing 0.1 M sodium
3 phosphate buffer, pH 6.0 and 0.13 mM EDTA mixed with methanol by a high-pressure gradient
4 system at a flow-rate of 1.2 ml/min (2 pumps, L-7100, Merck-Hitachi) in a step-gradient of 18%
5 methanol for 18 min and 38% methanol for the remainder of the 25-min run. Derivatized amino
6 acids (GABA, alanine, serine, threonine, glycine, taurine, glutamate, glutamine, aspartate, or
7 asparagine) were detected by a fluorescence detector (L-7480, Merck-Hitachi) with excitation at
8 340 nm and emission at 440 nm. Ten major amino acids, including GABA, were detected and
9 quantified. GABA levels were normalized to the alanine content, using alanine as an internal
10 reference.

11 **Evaluation of loss in immunoreactivity and mRNA in the rat brain *post mortem***

12 To evaluate the possible loss in immunoreactivity and mRNA post mortem, we performed an
13 experiment in which rat brains were exposed for different time intervals to elevated (16 °C)
14 temperature prior to histochemistry. For immunohistochemistry rat brains were perfused with
15 PBS (25 ml, room temperature) to remove blood cells and thus to avoid artefacts by
16 endogenous peroxidase activity. They were kept within their skulls 0, 8 and 24 h (N = 4 for each
17 group) and then fixed in 4 % PFA as described for the human brain samples. For *in situ*
18 hybridization a separate set of rat brains was obtained. These brains were not perfused and
19 removed after the same time intervals from their skulls and snap frozen in -70 °C isopentane.
20 For *in situ* hybridization and immunohistochemistry the same protocols as for the human
21 samples were used. A probe for rat GAD67
22 (GCAGGTTCTTGGAGGCCTGCCTCTCCCTGAAGGCGCTCAC; custom synthesized by
23 Microsynth, Balgach, Switzerland) was applied.

24 **Statistical analyses**

25 Data are presented as means \pm SEM. They were analyzed for normal distribution and equal
26 variances using GraphPad Prism software (Prism 5 for Macintosh, GraphPad Software Inc.,
27 San Diego, CA). Statistical analyses were done by Student's *t*-test for data with normal
28 distribution or Mann-Whitney test as a nonparametric test. Analysis of variance (ANOVA) was
29 used for multiple comparisons (rat studies). Statistical analysis of GAD67/dynorphin co-
30 distribution with clinical data was done for sclerotic and non-sclerotic specimens by analysis of
31 covariance (ANCOVA). GAD67/dynorphin co-distribution rating was defined as the dependent
32 variable and age, years after onset of epilepsy, age of seizure onset, number of anti-epileptic
33 drugs, degeneration score, granule cell dispersion and number of seizures per month as
34 covariates. ANCOVA was performed on SPSS 16.0 (SPSS Inc., Chicago, IL, USA).

RESULTS

Clinical variables of patients

Specimens were obtained from 44 TLE patients and 11 autopsy controls. Clinical variables are shown in Tables 1 and 2, respectively. Among the TLE patients 37 revealed hippocampal sclerosis, 7 were non-sclerotic. Patients with Ammon's horn sclerosis had a significantly higher granule cell dispersion rating than non-sclerotic patients ($P= 0.003$) but did not significantly differ in time of onset of epilepsy ($P< 0.450$), duration of epilepsy ($P= 0.227$), number of seizures/month ($P= 0.947$), number of antiepileptic drugs in treatment before surgery ($P=0.338$) or in GAD67/dynorphin co-distribution rating ($P= 0.746$). The age at surgery did not differ between non-sclerotic (mean \pm SEM: 32.6 ± 5.46) and sclerotic patients (35.4 ± 2.03) but was significantly higher in autopsy controls (52.5 ± 5.61 ; $P<0.01$).

Post mortem changes in GAD67 protein and mRNA levels in the rat

To examine the influence of time from death to fixation/snap freezing of the tissue we examined GAD67-IR and GAD67 mRNA levels in mossy fibers and granule cells, respectively at death and 8 and 24 h after storing the brains at 16°C. After 24 h, we observed a 28 % decrease in immunoreactivity and a 24 % decrease in mRNA levels (Fig. 1). The ratio of RODs GAD67/NSE in Western blotting was unchanged, although there was a 65 % reduction in ROD values per μ g protein for both NSE and GAD67 (data not shown). Interestingly, in the human brains ROD values/ μ g protein were identical for post mortem and epilepsy specimens, indicating a higher stability of proteins in the human brain than in rat brains at the indicated experimental conditions.

Distribution of GAD67 and dynorphin immunoreactivities. The distribution of GAD67-IR was heterogeneous in the TLE specimens. Strikingly, in most cases (38 of 44) labeling was considerably stronger in the terminal fields of mossy fibers (dentate hilus, stratum lucidum) than in areas associated with dense GABAergic axon terminals (e.g. the outer molecular layer of the dentate gyrus, axons of GABA neurons passing the CA1 stratum pyramidale) (Fig. 2A). In all cases with moderate to strong hippocampal sclerosis ($n = 36$), the inner molecular layer of the dentate gyrus, corresponding to the terminal area of sprouted mossy fibers, was also immunoreactive for GAD67 (Figs. 2A, 3A). In contrast, specimens without Ammon's horn sclerosis ($n = 8$) revealed labeling in the hilus and in the stratum lucidum of CA3 but not in the inner molecular layer of the dentate gyrus (Fig. 3D). Dense immunoreactivity was also present in the subiculum (Fig. 2D).

With the exception of four specimens, the distribution of GAD67-IR closely resembled that obtained for dynorphin-IR in adjacent sections. Labeling of mossy fibers in the hilus of the dentate gyrus, along the pyramidal layer in sector CA3 and the terminal field of mossy fibers in

1 the stratum lucidum was strikingly similar for both markers (Fig. 2A, B). In addition, bundles of
2 mossy fibers and plaque-like structures in the dentate hilus presumably originating from
3 degenerating mossy fibers were immunoreactive for GAD67 and dynorphin (Fig. 2A, B and 4 D-
4 F). In all specimens with Ammon's horn sclerosis, dynorphin-IR was also observed in the inner
5 molecular layer labeling terminals of sprouted mossy fibers (Figs. 2B, 3B, 4H; Houser et al,
6 1990). In non-sclerotic specimens, dynorphin-IR was restricted to the middle and outer segment
7 of the dentate molecular layer, where it presumably labeled afferent fibers of the perforant path
8 (Fig. 3E). Faint GAD67-IR was observed also in the terminal field of mossy fibers in post
9 mortem controls (not shown). In order to find possible differences in the labeling of mossy fibers
10 by GAD67 and to correlate these with the clinical data, we had assessed a rating of the co-
11 distribution of GAD67-IR with the mossy fiber marker dynorphin (Table 1).

21 Clinical variables were compared with the GAD67/dynorphin score by ANCOVA. Controlling for
22 the patient group (sclerotic, non-sclerotic) rating for GAD67/dynorphin co-labeling did not
23 correlate with age ($F_{(1,35)}=0.08$; $P=0.78$), duration of epilepsy ($F_{(1,35)}=2.50$; $P=0.12$), age of
24 seizure onset ($F_{(1,35)}=1.88$; $P=0.18$), number of medications ($F_{(1,35)}=2.17$; $P=0.15$), granule cell
25 dispersion ($F_{(1,35)}=2.18$; $P=0.15$) or degeneration rate ($F_{(1,35)}=0.44$; $P=0.51$). There was,
26 however, a significant correlation between GAD67/dynorphin co-labeling and number of
27 seizures per month ($F_{(1,35)}=4.91$; $P=0.03$).

34 **Vesicular GABA transporter (VGAT) and GAD65.** We used VGAT-IR to label GABA-ergic
35 nerve fibers. VGAT-IR was present throughout the hippocampal formation of TLE specimens
36 (Fig. 2E). It labeled thin varicose fibers in the molecular layer (preferentially in the outer
37 molecular layer), the hilus of the dentate gyrus, and throughout all segments of the
38 hippocampus (Figs. 2E, 3C). Axons passing through the dentate granule cell layer and through
39 residual parts of the pyramidal cell layers were labeled with the VGAT antibody in sclerotic
40 specimens (Fig. 2E). In the dentate molecular layer of sclerotic specimens the inner and outer
41 molecular layer were equally labeled for VGAT, presumably reflecting the labeling pattern of
42 sprouted interneurons (Mathern et al., 1995; Furtinger et al., 2001). In non-sclerotic specimens,
43 VGAT-IR was mostly restricted to the outer segment, where it labeled terminals of GABA-ergic
44 interneurons of the dentate hilus (Fig. 3F). In none of the specimens investigated, VGAT-IR
45 resembled that of dynorphin-IR outlining the terminal field of mossy fibers in the stratum lucidum
46 or mossy fiber bundles in the dentate hilus. GAD65-IR was weak and followed the pattern of
47 VGAT-IR and no labeling was observed in mossy fibers (Fig. 2F).

59 **Double immunofluorescence for GAD67 and dynorphin, and GAD67 and VGAT**

60 For unequivocally demonstrating expression of GAD67 in mossy fibers, we performed double
immunofluorescence labeling of GAD67 with the mossy fiber marker dynorphin and with VGAT
as a marker for GABA-ergic nerve fibers. As shown in Fig. 4, GAD67-IR was expressed

1
2 together with dynorphin-IR in mossy fiber terminals of the stratum lucidum of CA3 (Fig. 4A-C)
3 and in bundles of mossy fibers in the hilus of the dentate gyrus (Fig. 4D-F). In specimens with
4 Ammon's horn sclerosis, GAD67-IR and dynorphin-IR also co-labeled fibers in the inner but not
5 in the outer molecular layer of the dentate gyrus (Fig. 4G-I). In contrast, VGAT-IR was strong in
6 the inner and outer molecular layer (labeling terminals of GABA-ergic interneurons arising from
7 the hilus) (Fig. 4K), whereas GAD67-IR was enriched in the inner molecular layer compared
8 with the outer segment (Fig. 4J). GAD67, present in mossy fibers, also demonstrated strong
9 labeling in the hilus (Fig. 4J), which contrasted with the weak VGAT-IR in this area (Fig 4K).

16 **GAD67 immunoblotting**

17 To characterize GAD67-IR in the brain specimen and for obtaining a quantitative estimate of the
18 increase in GAD67 levels in TLE specimens, we performed immunoblotting experiments
19 comparing GAD67 levels in the dentate gyrus of 8 TLE and 8 post mortem specimens. Using
20 the same monoclonal GAD67 antibody as for the immunohistochemical studies, we observed
21 single bands migrating around 67 kDa both in control and epileptic tissue, demonstrating the
22 specificity of immunolabelling (Fig. 5A). NSE was used as a reference protein. GAD67/NSE
23 ratios were about 20 times higher ($p < 0.0001$) in TLE specimens ($n = 8$) than in controls ($n = 8$),
24 indicating a remarkable increase in GAD67 protein levels in the epileptic dentate gyrus (Fig.
25 5B).

34 ***In situ* hybridization of GAD67 mRNA**

35 For obtaining further evidence for GAD67 expression in granule cells/mossy fibers we
36 performed *in situ* hybridization for GAD67 mRNA. As shown in Fig. 6, GAD67 mRNA was
37 detected in the granule cell layer of all TLE and post-mortem specimens investigated. In
38 representative samples of sclerotic TLE ($n = 33$) and non-sclerotic specimens ($n = 5$),
39 concentrations of GAD67 mRNA were significantly increased compared to post-mortem control
40 specimens ($n = 9$): Mean % of control \pm SEM of sclerotic specimens: $179.0 \pm 18.25\%$; $P <$
41 0.0002 ; range 107–328 %; non-sclerotic specimens: $163 \pm 25.9\%$; $P < 0.022$; range 92 -250 %.
42 When correcting in the sclerotic specimens the values to account for cell loss in the granule cell
43 layer, mRNA levels were $361.9 \pm 31.38\%$ of control ($P < 0.0002$; range: 180–558%). There was
44 no significant difference between the increases in mRNA levels in the sclerotic vs. non-sclerotic
45 cases ($P < 0.74$).

56 **Increased concentrations of GABA in the dentate gyrus**

57 For obtaining evidence for a change in GABA synthesis in the area of mossy fibers, we
58 determined the concentrations of ten amino acids including GABA in sections of the dentate
59 gyrus. To correct for variations in tissue concentrations, we calculated GABA levels as the ratio
60 of GABA/alanine, using alanine as an internal standard. Mean ratios \pm SEM were 1.65 ± 0.075

(n = 10; range: 1.35 to 2.00) in TLE and 0.66 ± 0.088 (n = 6) in autopsy control specimens, reflecting a highly significant ($P < 0.0001$) increase (152%, range: 0.32 to 0.90) in GABA levels in the TLE specimens. GABA/amino acid ratios were also significantly increased when calculated for either of the other amino acids determined concomitantly (serine, threonine, glycine, taurine, glutamate, glutamine, aspartate or asparagine).

DISCUSSION

Our study provides the first evidence for pronounced expression of one of the two key enzymes in GABA synthesis, GAD67, in mossy fibers, a prominent glutamatergic fiber tract of the hippocampus. This expression was demonstrated in specimens obtained at surgery from patients with TLE using conventional immunohistochemistry and double immunofluorescence. GAD67 was co-localized together with the mossy fiber marker dynorphin to bundles of mossy fibers of the dentate hilus, to mossy fiber terminals in the stratum lucidum, and to the inner molecular layer aberrantly innervated by mossy fiber sprouting in TLE patients with Ammon's horn sclerosis. In addition we observed expression of GAD67 mRNA in dentate granule cells. Our findings also indicate an increase in the expression of GAD67 protein, accompanied by increases in GAD67 mRNA and GABA levels in the area of the dentate gyrus. Direct comparisons, however, of freshly removed surgical tissue with post mortem controls have certainly to be done with caution. In particular, GABA levels may be sensitive to post mortem metabolism. Indeed, an experiment in rats mimicking the post mortem autolysis of the human tissue revealed a roughly 25 - 30 % decrease in GAD67 mRNA and protein within 24 h (the longest post mortem interval in the human specimens was 16 h). In spite, taken the 80 to 260 % increases in granule cell mRNA levels and the 2000 % increases in GAD67 protein in the dentate gyrus an induction of GAD67 expression in TLE is still likely. This assumption for the epileptic human hippocampus is supported by the recent studies in animal models of TLE showing pronounced expression (and up-regulation) of GAD67 but not of VGAT mRNA and protein in granule cells/mossy fibers of the dentate gyrus (Szabo et al., 2000; Sperk et al., 2003).

Interestingly, in GAD67 mRNA expression is rapid but transient in the rat epilepsy model (Schwarzer and Sperk, 1995; Szabo et al., 2000). This may explain the relatively modest increases in mRNA levels compared with the strong increases in GAD67 protein in the human specimens. The expression of GAD67 protein may also be triggered by repeated seizures. This is indicated by the correlation of the number of seizures/month and the GAD67/dynorphin co-

1
2 labeling. It implies that GAD67 expression in mossy fibers may be a compensatory mechanism
3 or a long-term effect of repeated seizures.
4

5
6
7 The relatively poor co-labeling of GAD67-IR with VGAT-IR in GABA-ergic neuron terminals was
8 also interesting, but may be explained by a specific and dramatic up-regulation of GAD67-IR in
9 mossy fibers with a concurrent loss of GABA interneurons. In contrast to GAD67, GAD65
10 appears not to be expressed in mossy fibers. Thus, using an antibody that preferentially detects
11 GAD65, Mathern and colleagues (Mathern et al., 1999) reported a distribution of GAD65 that
12 correlated with the distribution of GABA-ergic axons and neurons (e.g. labeling the outer
13 molecular layer of the dentate gyrus) but not with that of mossy fibers. In our specimens, we
14 observed a similar pattern of GAD65-IR, corresponding to the distribution of VGAT-IR but not
15 that of dynorphin-IR (see Pirker et al., 2001, not shown here) and indicating that GAD65 is
16 expressed in the axons of GABA-ergic neurons but not in mossy fibers. Since GAD65 seems to
17 be more closely related to synaptic transmission than GAD67 (Soghomonian and Martin, 1998),
18 the finding that GAD67 but not GAD65 is up-regulated in mossy fibers points to a preferentially
19 non-synaptic role of this mechanism.
20
21
22
23
24
25
26
27

28
29 Although GAD67 and GAD65 are generally expressed together in GABA-ergic neurons, the two
30 enzymes also present distinct differences (Mathern et al., 1999). Whereas the activity of GAD65
31 is regulated by its affinity to the cofactor pyridoxal phosphate, GAD67 has the cofactor tightly
32 bound, and its activity is regulated by changes in mRNA expression. GAD65 has also been
33 suggested to be preferentially targeted to nerve endings and to be responsible for synthesis of
34 GABA stored in vesicles, whereas GAD67 is more ubiquitously distributed within neurons and
35 may be associated with the synthesis of GABA released by non-vesicular mechanisms
36 (Esclapez et al., 1994; Soghomonian and Martin, 1998).
37
38
39
40
41
42
43

44 The co-existence of GABA with other transmitters is not unique. Neurons expressing GAD67,
45 VGAT, and the vesicular glutamate transporter have been recently identified in the
46 anterioventral periventricular nucleus of female rats, indicating that these neurons have a dual
47 glutamatergic/GABA-ergic phenotype that preconditions them for exocytotic release of both
48 neurotransmitters (Ottem et al., 2004).
49
50
51
52

53 Retinal amacrine cells provide another well-characterized example of GABA co-localizing with
54 another classical neurotransmitter in the same neurons. Such cells contain GAD67, but not
55 GAD65, in addition to choline acetyltransferase (Brandon and Criswell, 1995). Whereas
56 acetylcholine release from amacrine cells is highly Ca^{2+} -dependent and involves exocytosis,
57 GABA is released from the same cells by Ca^{2+} -independent reverse transport (O'Malley et al.,
58 1992). In contrast to acetylcholine, radiolabeled GABA also does not accumulate in the synaptic
59
60

1 vesicles of amacrine cells, indicating that although the cells express GAD67, they do not contain
2 a vesicular GABA transporter (O'Malley and Masland, 1989; O'Malley et al., 1992).
3
4

5
6
7 A possible route of GABA release from mossy fibers may also involve reverse transport.
8 Granule cells contain the cell membrane GABA transporter GAT-1 (Frahm et al., 2000; Sperk et
9 al., 2003), and no immunohistochemical evidence for expression of VGAT in granule cells has
10 been reported to date (Sperk et al., 2003; Boulland et al., 2007). The direction of GABA
11 transport has been well documented to be highly dependent on actual intracellular
12 concentrations of Na⁺ and GABA (Schwartz, 1987; Attwell et al., 1993; Koch and Magnusson,
13 2009). Thus, even minute increases in intracellular GABA concentration, caused by the
14 extremely high expression of GAD67 in TLE or a rise in intracellular Na⁺ concentration during
15 epileptiform discharges, will obligatorily induce outward GABA transport in the epileptic
16 hippocampus (During et al., 1995; Wu et al., 2001). GABA released from granule cell dendrites
17 may then act on inhibitory GABA_A receptors present at high concentrations especially in the
18 molecular layer of the epileptic hippocampus. Clearly this process may represent an
19 endogenous anticonvulsive mechanism that would be especially active during acute epileptic
20 events.
21
22
23
24
25
26
27
28
29
30

31 There is, however, also clear evidence for Ca⁺⁺ dependent release of GABA at mossy fiber
32 terminals. Stimulation of granule cells results in monosynaptic GABA_A receptor-mediated
33 synaptic signals in the CA3 pyramidal neurons of normal guinea pigs (Walker et al., 2001) and
34 kindled rats (Gutierrez and Heinemann, 2001). These signals have properties typical of those of
35 mossy fibers; they are NMDA-receptor independent and induce long-term potentiation upon
36 repeated stimulation (Walker et al., 2001). On the other hand, these findings have not been
37 replicated in 3 weeks old rats in which exocytotic GABA release from mossy fibers could not be
38 provoked (Uchigashima et al., 2007). Irrespective of the actual mechanism (exocytotic release
39 of GABA at mossy fiber-CA3 synapses or reverse transport of GABA, e.g. at granule cell
40 dendrites, or both), increased extracellular availability of GABA may serve as an endogenous
41 anticonvulsive principle that helps terminate seizures.
42
43
44
45
46
47
48
49
50

51 Another function of the extremely high concentration of GAD67 within granule cells/mossy fibers
52 may be to convert excessive glutamate released from and taken up again by mossy fiber
53 terminals during epileptic seizures to non-toxic GABA. This mechanism would prevent reverse
54 transport of glutamate from mossy fibers and diminish excitotoxic cell death.
55
56
57
58

59 Further insight into the expression and functional role of GAD67 in mossy fibers has still to be
60 obtained by electron microscopic studies in tissues obtained at surgery. It would be important to
investigate in human TLE tissue a possible role of GABA secreted from mossy fibers or from
granule cell dendrites on GABA_A and GABA_B receptors by electrophysiology. A major drawback

1
2 of this study is also the comparison of histochemical data obtained from fresh surgical tissue
3 with that of post mortem tissue. Although we attempted to control for decay of histochemical
4 markers by mimicking post mortem changes in the rat brain, changes in rat brain and human
5 tissue could vary considerably.
6
7
8
9

10 11 12 13 **ACKNOWLEDGEMENTS**

14 We thank Lisi Gasser for technical assistance and Prof. H. Hörtnagl for discussion.
15
16
17
18
19
20
21
22
23
24
25
26
27
28
29
30
31
32
33
34
35
36
37
38
39
40
41
42
43
44
45
46
47
48
49
50
51
52
53
54
55
56
57
58
59
60

For Peer Review

REFERENCES

- 1
2
3
4
5 Attwell D, Barbour B, Szatkowski M. 1993. Nonvesicular release of neurotransmitter. *Neuron*
6 11:401–47.
7
8
9 Boulland JL, Ferhat L, Tallak Solbu T, Ferrand N, Chaudhry FA, Storm-Mathisen J, Esclapez M.
10 2007. Changes in vesicular transporters for gamma-aminobutyric acid and glutamate
11 reveal vulnerability and reorganization of hippocampal neurons following pilocarpine-
12 induced seizures. *J Comp Neurol* 503:466–485.
13
14
15 Bramham CR, Torp R, Zhang N, Storm-Mathisen J, Ottersen OP. 1990. Distribution of
16 glutamate-like immunoreactivity in excitatory hippocampal pathways: a semiquantitative
17 electron microscopic study in rats. *Neuroscience* 39:405–417.
18
19
20 Brandon C, Criswell MH. 1995. Displaced starburst amacrine cells of the rabbit retina contain
21 the 67-kDa isoform, but not the 65-kDa isoform, of glutamate decarboxylase. *Vis Neurosci*
22 12:1053–1061.
23
24
25 Chaudhry FA, Reimer RJ, Bellocchio EE, Danbolt NC, Osen KK, Edwards RH, Storm-Mathisen
26 J. 1998. The vesicular GABA transporter, VGAT, localizes to synaptic vesicles in sets of
27 glycinergic as well as GABAergic neurons. *J Neurosci* 18:9733–950.
28
29
30 Davies KG, Hermann BP, Dohan FCJ, Foley KT, Bush AJ, Wyler AR. 1996. Relationship of
31 hippocampal sclerosis to duration and age of onset of epilepsy, and childhood febrile
32 seizures in temporal lobectomy patients. *Epilepsy Res* 24:119–126.
33
34
35 During MJ, Ryder KM, Spencer DD. 1995. Hippocampal GABA transporter function in temporal-
36 lobe epilepsy. *Nature* 376:174–17.
37
38
39 Esclapez M, Tillakaratne NJ, Kaufman DL, Tobin AJ, Houser CR. 1994. Comparative
40 localization of two forms of glutamic acid decarboxylase and their mRNAs in rat brain
41 supports the concept of functional differences between the forms. *J Neurosci* 14:1834–
42 155.
43
44
45 Frahm C, Engel D, Piechotta A, Heinemann U, Draguhn A. 2000. Presence of gamma-
46 aminobutyric acid transporter mRNA in interneurons and principal cells of rat
47 hippocampus. *Neurosci Lett* 288:175–18.
48
49
50 Furtinger S, Pirker S, Czech T, Baumgartner C, Ransmayr G, Sperk G. 2001. Plasticity of Y1
51 and Y2 receptors and neuropeptide Y fibers in patients with temporal lobe epilepsy. *J*
52 *Neurosci* 21:5804–5812.
53
54
55 Gutierrez R, Heinemann U. 2001. Kindling induces transient fast inhibition in the dentate gyrus--
56 CA3 projection. *Eur J Neurosci* 13:1371–139.
57
58
59 Houser CR, Esclapez M. 1994. Localization of mRNAs encoding two forms of glutamic acid
60 decarboxylase in the rat hippocampal formation. *Hippocampus* 4:530–45.
Houser CR, Miyashiro JE, Swartz BE, Walsh GO, Rich JR, Delgado-Escueta AV 1990 Altered
patterns of dynorphin immunoreactivity suggest mossy fiber reorganization in human
hippocampal epilepsy. *J Neurosci*, 10:267–282.

- 1
2 Koch U, Magnusson AK. 2009. Unconventional GABA release: mechanisms and function. *Curr*
3
4 *Opin Neurobiol* 19:305–310.
- 5 Mathern GW, Babb TL, Pretorius JK, Leite JP 1995 Reactive synaptogenesis and neuron
6
7 densities for neuropeptide Y, somatostatin, and glutamate decarboxylase
8
9 immunoreactivity in the epileptogenic human fascia dentata. *J Neurosci*. 15:3990–4004.
- 10 Mathern GW, Mendoza D, Lozada A, Pretorius JK, Dehnes Y, Danbolt NC, Nelson N, Leite JP,
11
12 Chimelli L, Born DE, Sakamoto AC, Assirati JA, Fried I, Peacock WJ, Ojemann GA,
13
14 Adelson PD. 1999. Hippocampal GABA and glutamate transporter immunoreactivity in
15
16 patients with temporal lobe epilepsy. *Neurology* 52:453–72.
- 17 Mikkonen M, Soininen H, Kalvianen R, Tapiola T, Ylinen A, Vapalahti M, Paljarvi L, Pitkanen A.
18
19 1998. Remodeling of neuronal circuitries in human temporal lobe epilepsy: increased
20
21 expression of highly polysialylated neural cell adhesion molecule in the hippocampus and
22
23 the entorhinal cortex. *Ann Neurol* 44:923–934.
- 24 O'Malley DM, Masland RH. 1989. Co-release of acetylcholine and gamma-aminobutyric acid by
25
26 a retinal neuron. *Proc Natl Acad Sci U S A* 86:3414–3418.
- 27 O'Malley DM, Sandell JH, Masland RH. 1992. Co-release of acetylcholine and GABA by the
28
29 starburst amacrine cells. *J Neurosci* 12:1394–1408.
- 30 Ottem EN, Godwin JG, Krishnan S, Petersen SL. 2004. Dual-phenotype GABA/glutamate
31
32 neurons in adult preoptic area: sexual dimorphism and function. *J Neurosci* 24:8097–
33
34 8105.
- 35 Pirker S, Czech T, Baumgartner C, Maier H, Novak K, Furtinger S, Fischer-Colbrie R, Sperk G.
36
37 2001. Chromogranins as markers of altered hippocampal circuitry in temporal lobe
38
39 epilepsy. *Ann Neurol* 50:216–226.
- 40 Pirker S, Gasser E, Czech T, Baumgartner C, Schuh E, Feucht M, Novak K, Zimprich F, Sperk
41
42 G. 2009. Dynamic up-regulation of prodynorphin transcription in temporal lobe epilepsy.
43
44 *Hippocampus* 19:1051–1054.
- 45 Sandler R, Smith AD. 1991. Coexistence of GABA and glutamate in mossy fiber terminals of the
46
47 primate hippocampus: an ultrastructural study. *J Comp Neurol* 303:177–92.
- 48 Schwartz EA. 1987. Depolarization without calcium can release gamma-aminobutyric acid from
49
50 a retinal neuron. *Science* 238:350–35.
- 51 Schwarzer C, Sperk G. 1995. Hippocampal granule cells express glutamic acid decarboxylase-
52
53 67 after limbic seizures in the rat. *Neuroscience* 69:705–79.
- 54 Sloviter RS, Dichter MA, Rachinsky TL, Dean E, Goodman JH, Sollas AL, Martin DL. 1996.
55
56 Basal expression and induction of glutamate decarboxylase and GABA in excitatory
57
58 granule cells of the rat and monkey hippocampal dentate gyrus. *J Comp Neurol* 373:593–
59
60 618.
- Soghomonian JJ, Martin DL. 1998. Two isoforms of glutamate decarboxylase: why? *Trends*
Pharmacol Sci 19:500–505.

- 1
2 Sperk G, Schwarzer C, Heilman J, Furtinger S, Reimer RJ, Edwards RH, Nelson N. 2003.
3 Expression of plasma membrane GABA transporters but not of the vesicular GABA
4 transporter in dentate granule cells after kainic acid seizures. *Hippocampus* 13:806–815.
5
6 Sutula T, Cascino G, Cavazos J, Parada I, Ramirez L. 1989. Mossy fiber synaptic
7 reorganization in the epileptic human temporal lobe. *Ann Neurol* 26:321–330.
8
9 Szabo G, Kartarova Z, Hoernagl B, Somogyi R, Sperk G. 2000. Differential regulation of adult
10 and embryonic glutamate decarboxylases in rat dentate granule cells after kainate-
11 induced limbic seizures. *Neuroscience* 100:287–295.
12
13 Uchigashima M, Fukaya M, Watanabe M, Kamiya H. 2007 Evidence against GABA release
14 from glutamatergic mossy fiber terminals in the developing hippocampus. *J Neurosci*,
15 27:8088–8100.
16
17 Walker MC, Ruiz A, Kullmann DM. 2001. Monosynaptic GABAergic signaling from dentate to
18 CA3 with a pharmacological and physiological profile typical of mossy fiber synapses.
19 *Neuron* 29:703–15.
20
21 Wiebe S, Blume WT, Girvin JP, Eliasziw M. 2001. A randomized, controlled trial of surgery for
22 temporal-lobe epilepsy. *N Engl J Med* 345:311–318.
23
24 Wu Y, Wang W, Richerson GB. 2001. GABA transaminase inhibition induces spontaneous and
25 enhances depolarization-evoked GABA efflux via reversal of the GABA transporter. *J*
26 *Neurosci* 21:2630–269.
27
28
29
30
31
32
33
34
35
36
37
38
39
40
41
42
43
44
45
46
47
48
49
50
51
52
53
54
55
56
57
58
59
60

Patient No	Age	Age at onset of epilepsy (years)	Surgery (years after onset of epilepsy)	Early risk factors	Medications	No of Seizures /month	Vegetation rating	Granule cell dispersion rating	GAD67/dyn score
Sclerotic specimens									
N3/99	27	22	5	Febr.s. (13 m)	LTG	4	2	2 / D	2.7
N5/99	60	13	47	no	CBZ, VGB	4.5	4	2	3.0
N6/99	33	23	10	Febr.s. (18 m)	CBZ, LTG	5.5	4	2	3.0
N10/99	33	1	32	no	CBZ, TGB, VGB	4	3	1	2.5
N15/99	30	23	7	trauma (4 y)	CBZ	5	2	1	2.8
N16/99	51	31	20	no	CBZ	4.5	3	3	2.7
N3/00	47	25	22	no	CBZ, TPM	5	4	1	2.2
H2/01	39	12	27	Febr.s. (3 y)	TPM, OXC	12.5	4	3	2.3
M8/01	38	4	34	Febr.s. (9 m)	OXC	3.5	4	2	2.2
N1/01	41	1	40	Febr.s. (12 m)	CBZ	50	2	2/D	0.8
N2/01	17	1	16	trauma (1y)	OXC, TPM	18	4	3/D	0.8
N3/01	22	3	19	no	LTG, TPM	7.5	2	1/D	3.0
N5/01	35	20	15	trauma (14 y)	CBZ	2	2	3/D	2.0
M3/02	39	35	4	no	OXC	?	3	2/D	3.0
M5/02	16	9	7	Febr.s. (18 m)	OXC	2	4	0	2.3
M13/02	65	14	51	no	CLB, PRD, OXC	3	2	0	3.0
M15/02	29	25	4	trauma (7 y)	PHT, LEV	0.2	3	0	1.7
M17/03	55	27	28	meningitis (1 y)	CBZ, LTG	1.5	3	0	2.8
M21/03	35	2	33	Febr.s. (8 m), meningitis (3y)	CBZ	4.5	4	2	1.2
M22/03	48	6	42	no	LEV, PHT, GBP	1	3	2	1.4
M24/03	37	6	31	trauma (baby)	LTG, CLB	1.5	4	3	1.0
M25/03	9	4	5	Febr.s. (2 y)	OXC	3	2	0	3.0
M26/03	9	3	6	Febr.s. (1 y)	VPA	8	3	0	3.0
E18	29	26	3	trauma (21 y)	CBZ, GBP	49	3	2	3.0
E19	37	20	17	Febr.s. (1 y)	PHT, GBP	24	4	1	0.6
E22	37	12	25	no	PHT, GBP	10.5	2	1	2.5
E25	33	1	32	meningitis (1 y)	CBZ	0.5	4	0	2.5
E30	45	1	44	Febr.s. (1 y)	PRD	4.5	2	3/D	1.5
E32	31	3	28	no	CBZ, PHT	15	4	0	3.0
E34	29	11	18	no	CBZ, VPA	4.5	3	2	1.8
E35	25	9	16	no	CBZ, VPA	12.5	2	1	1.8
E36	41	25	16	no	PHT	32	2	0	1.3
E39	32	14	18	Febr.s. (4 y)	CBZ, VGB	2.5	3	2	2.5
E40	40	6	34	trauma (2 y)	CBZ	28	3	2	1.0
E41	45	38	7	trauma (25 y)	PHT, OXC, CLB	4	3	2	3.0
E45	27	6	21	Febr.s. (6 m), trauma (4 y)	CBZ	3.5	3	3/D	1.0
N2/99	43	0	43	no	CBZ	2	2	1	2.0
Non-sclerotic and modestly sclerotic specimens									
N9/99	35	10	25	no	CBZ, TPM, CLB barbexaclon,	4.5	0	0	2.0
G1/00	56	45	11	no	OXC	17	0	0	0
N13/99	48	36	12	no	CBZ	2	0	1	3.0
K6/00	17	11	6	trauma (10 y)	FBM, OXC, CLB	7	1	0	2.5
K10/01	26	2	24	no	CBZ	2.5	1	0	1.8
H1/02	24	7	17	no	OXC, TPM, LEV	3.5	0	0	2.8
E27	22	13	9	no	LTG, VGB	7	0	0	2.0

1
2
3
4 Table 1: Clinical data of the 44 patients included in the immunohistochemical study: comparison
5 with rating for codistribution of GAD67 and dynorphin in TLE patients with and without
6 hippocampal sclerosis. For rating scales see Methods. Abbreviations: Early risk factors: Febr.s.,
7 febrile seizures; in parenthesis the age of occurrence in years (y) or months (m) is given.
8 Medication: CBZ, carbamazepine; CLB, clobazam; FBM, felbamate; GBP, gabapentin; LTG,
9 lamotrigine; LEV, levetiracetam; OXC, oxcarbazepine; PHT, phenytoin; PRD, primidone; TGB
10 tiagabin, TPM, topiramate; VPA, valproic acid; VGB, vigabatrine. For rating of degeneration and
11 granule cell dispersion see Methods section. GAD67/dyn score: score for co-distribution of
12 GAD67- and dynorphin-IR in terminal areas of mossy fibers (dentate gyrus, stratum lucidum
13 CA3, inner molecular layer of the dentate gyrus in sclerotic cases). These values represent
14 means of ratings obtained for the three areas by two independent observers. D in column
15 granule cell dispersion denotes double layer.
16
17
18
19
20
21
22
23
24
25
26
27
28
29
30
31
32
33
34
35
36
37
38
39
40
41
42
43
44
45
46
47
48
49
50
51
52
53
54
55
56
57
58
59
60

Patient No	Age at death	Sex	Cause of death	Time to autopsy
Controls				
C1	28	m	pneumonia	16
C4	95	m	pulmonary embolism	8
C6	58	m	pharynx cancer	11
C7	54	m	liver cirrhosis	8
C8	42	m	leucemia	9
C9	46	m	melanoma	13.5
C10	51	f	breast cancer	15
C11	76	f	myocardal infarct	8
C15	44	m	lymphom	12.5
C16	41	m	liver cirrhosis	15.5
C18	42	m	stomach cancer	11

Table 2: Clinical data of post mortem controls.

Legends to Figures

FIGURE 1. Influence of post mortem time on GAD67-IR and mRNA levels in the rat brain. Rats were killed and decapitated. Their skulls were kept for 0, 8 and 24 h at 16°C. Their brains were then removed and either immersion fixed with paraformaldehyde for subsequent immunohistochemistry or snap frozen for in situ hybridization.

In A, D and G GAD67-IR is shown in the dentate gyrus at the post mortem intervals of 0, 8 and 24 h, respectively. In B, E, H, GAD67-IR is shown in the prefrontal cortex region revealing survival of GAD67-IR neurons at the same intervals. In C, F, I GAD67 mRNA is shown at post mortem intervals of 0, 8 and 24 hrs. In J and K relative optical density (ROD) values are shown for the mossy fibers in the tip of the hilus (A, D, G) and for the granule cell layer (C, F, I), respectively. The numbers of animals per group were 4. Statistical analysis was done by ANOVA with Bonferoni post hoc test. *P* refers to the non-exposed (0 h) group.

FIGURE 2. Distribution of GAD67-, dynorphin-, VGAT- and NeuN-IR in the hippocampus of a TLE patient with Ammon's horn sclerosis (A–C, E, F; case E18) and of GAD67-IR in a specimen without hippocampal sclerosis (D; case K10/01). In the specimen with Ammon's horn sclerosis, NeuN-IR (C) reveals cell losses in the hilus and in sectors CA1 and CA3, whereas the subiculum (S) and the dentate granule cell layer are largely preserved. Dynorphin-IR (B) and GAD67-IR (A) mainly followed the pattern of the terminal field of mossy fibers (hilus of the dentate gyrus, stratum lucidum) and labeled the inner molecular layer (iml), which is aberrantly innervated by mossy fibers (mf). GAD67-IR was also present in the subiculum and extended (in contrast to dynorphin-IR) from the stratum lucidum (s. luc) to the stratum pyramidale of sector CA1 (there labeling fibers of GABA neurons). VGAT-IR (E) and GAD65-IR (F) revealed an entirely different labeling pattern in adjacent sections of the same (sclerotic) specimen reflecting the distribution of fibers originating from GABA-ergic interneurons. In contrast to dynorphin-IR and GAD67-IR VGAT-IR (E) and GAD65-IR (F) are faint in all terminal areas of mossy fibers, but label GABA-ergic fibers e.g. in the (inner and outer) molecular layer, in the stratum pyramidale CA1 and in the subiculum (E, F). Presumably due to neurodegeneration, the dentate hilus is weakly labeled for both markers (E, F). In D GAD67-IR is shown for a specimen without hippocampal sclerosis. It reveals a similar labeling pattern as the sclerotic specimen, except that the terminal area of sprouted mossy fibers in the inner dentate molecular layer lacks GAD67-IR. Presumably due to the lack of neurodegeneration, labeling of GABA neurons in the sector CA1 is also more prominent than in the sclerotic specimen. Arrowheads in A, B, D, E and F denote the borders between the stratum lucidum CA3 and stratum pyramidale CA2. Scale bar: 1mm.

FIGURE 3. Distribution of GAD67-IR, dynorphin-IR, and VGAT-IR in the molecular layer of the dentate gyrus of TLE patients with (A–C; patient E41) and without (D–F; patient E27) Ammon's

1
2 horn sclerosis. Dynorphin-IR serves as a specific marker for mossy fibers. VGAT labels the
3 axons of GABA interneurons. In the specimen with Ammon's horn sclerosis, the inner (iml) but
4 not the outer molecular layer (oml) is intensely labeled for GAD67 (A) and dynorphin (B),
5 whereas VGAT-IR labels the inner and the outer molecular layer equally. In the non-sclerotic
6 specimen, labeling of the iml by GAD67 and dynorphin is absent (D, E). Dynorphin-IR in the
7 middle and outer molecular layer (oml) presumably labels axon terminals of the perforant path
8 (E). In the outer molecular layer, VGAT-IR axons of hilar GABA neurons terminate and can be
9 well seen in the non-sclerotic specimen (F). Abbreviation: h, hilus, gc, granule cells. Scale bar:
10 100 μm .
11
12
13
14
15
16
17

18 **FIGURE 4.** Double immunofluorescence for GAD67 and the mossy fiber marker dynorphin in
19 terminal areas of mossy fibers (A–I) and of GAD67 and VGAT in GABAergic fibers of the
20 dentate gyrus (J–L) in sections from patients with hippocampal sclerosis. A–C shows co-labeling
21 of the stratum lucidum CA3 with GAD67- and dynorphin-IR (patient E18); D–F depicts co-
22 labeling of mossy fiber bundles in the dentate hilus (h) with GAD67-IR and dynorphin-IR (patient
23 E18). In G–I labeling of the dentate molecular layer of a sclerotic specimen is shown for
24 GAD67- and dynorphin-IR (case E41). Note co-labeling of GAD67 with the mossy fiber marker
25 dynorphin in the inner but not outer molecular layer (this is the terminal area of sprouted mossy
26 fibers in hippocampal sclerosis). On the other hand, VGAT a marker of GABA-ergic neurons
27 labels the outer molecular layer (K, L). Labeling for GAD67-IR again is strong in the inner (J, L)
28 and faint in the outer (J) molecular layer.
29
30
31
32
33
34
35

36 Scale bars: in C for A–C: 200 μm ; in F for D–F: 50 μm , in I and L for G–L: 200 μm .
37
38

39 **FIGURE 5.** Immunoblots of dentate gyrus tissue from TLE patients. In A, a representative
40 immunoblot of four arbitrarily selected, snap-frozen specimens from TLE patients (coded with
41 E1 to E4) and post-mortem controls (C1 to C4) is shown. The blots were consecutively
42 incubated with a monoclonal GAD67 antibody and an antibody for neuron-specific enolase
43 (NSE). Single bands were observed for GAD67 both in control and in TLE tissue. Panel B
44 depicts the ratios of ROD values obtained for GAD67 and NSE. ***Statistically different from
45 controls ($p < 0.0001$) using the two-tailed Student's t-test.
46
47
48
49
50
51

52 **FIGURE 6.** GAD67 mRNA. Autoradiographs of sections from the hippocampus of a post
53 mortem control (A), a TLE specimen with (B, case N 10/99) and one without hippocampal
54 sclerosis (C, case G1/00). Note the pronounced up-regulation of GAD67 mRNA in dentate
55 granule cells equally in the sclerotic and in the non-sclerotic specimen. For quantification see
56 text.
57
58
59
60

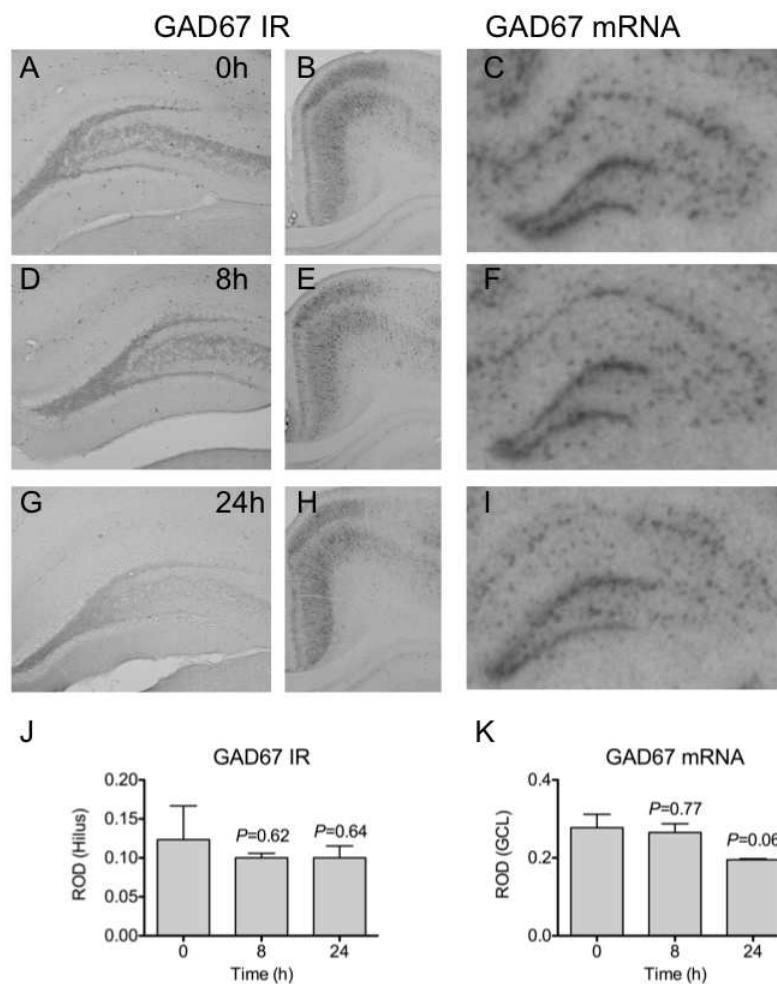


FIGURE 1. Influence of post mortem time on GAD67-IR and mRNA levels in the rat brain. Rats were killed and decapitated. Their skulls were kept for 0, 8 and 24 h at 16°C. Their brains were then removed and either immersion fixed with paraformaldehyde for subsequent immunohistochemistry or snap frozen for in situ hybridization.

In A, D and G GAD67-IR is shown in the dentate gyrus at the post mortem intervals of 0, 8 and 24 h, respectively. In B, E, H, GAD67-IR is shown in the prefrontal cortex region revealing survival of GAD67-IR neurons at the same intervals. In C, F, I GAD67 mRNA is shown at post mortem intervals of 0, 8 and 24 hrs. In J and K relative optical density (ROD) values are shown for the mossy fibers in the tip of the hilus (A, D, G) and for the granule cell layer (C, F, I), respectively. The numbers of animals per group were 4. Statistical analysis was done by ANOVA with Bonferoni post hoc test. P refers to the non-exposed (0 h) group.

264x352mm (72 x 72 DPI)

1
2
3
4
5
6
7
8
9
10
11
12
13
14
15
16
17
18
19
20
21
22
23
24
25
26
27
28
29
30
31
32
33
34
35
36
37
38
39
40
41
42
43
44
45
46
47
48
49
50
51
52
53
54
55
56
57
58
59
60

For Peer Review

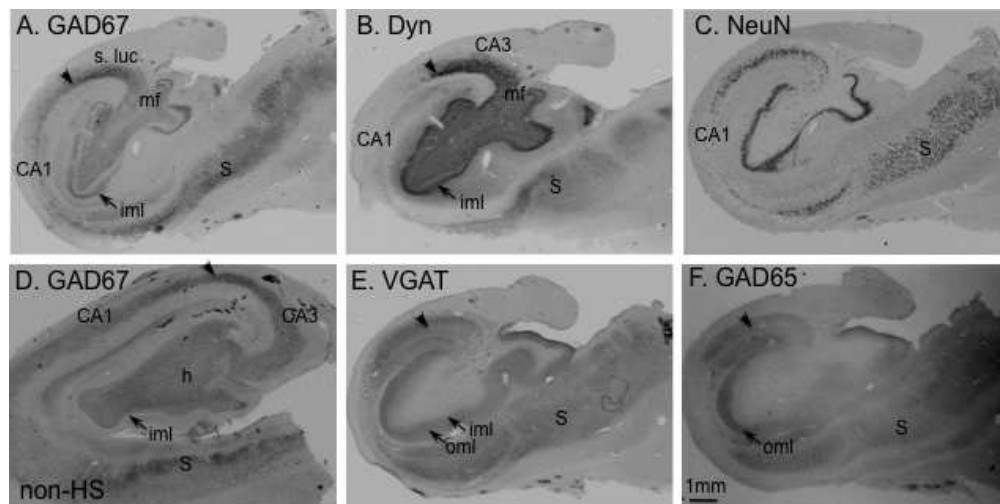
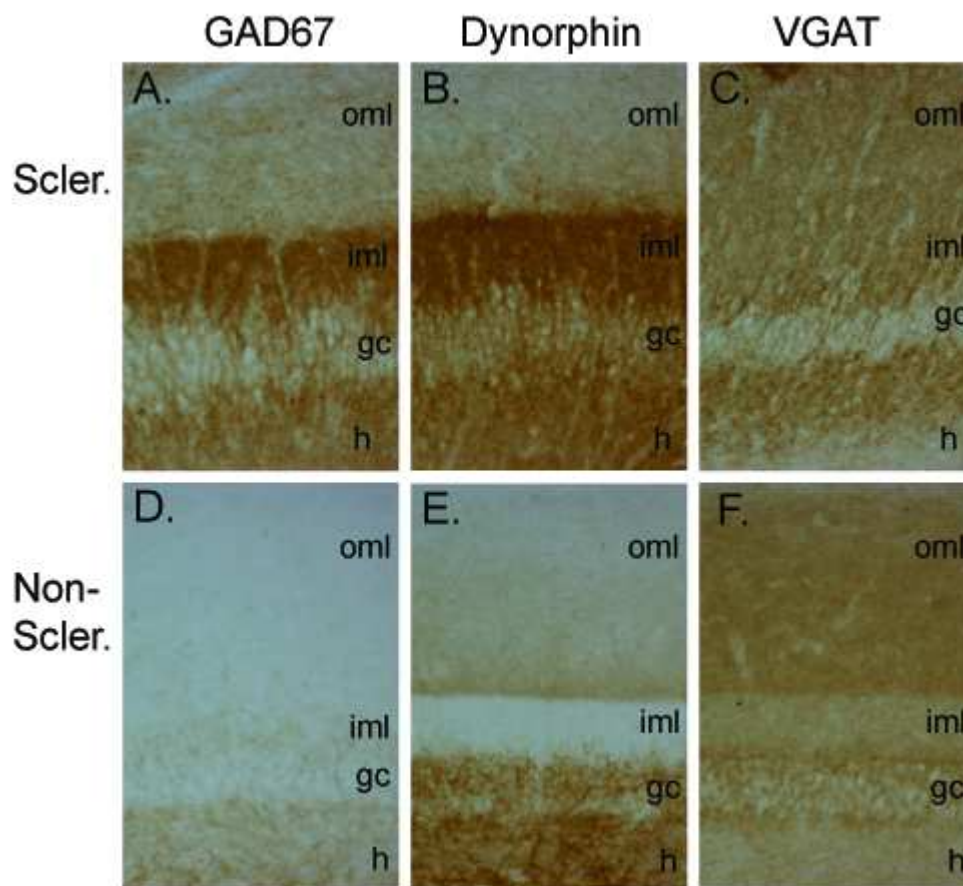


FIGURE 2. Distribution of GAD67-, dynorphin-, VGAT- and NeuN-IR in the hippocampus of a TLE patient with Ammon's horn sclerosis (A-C, E, F; case E18) and of GAD67-IR in a specimen without hippocampal sclerosis (D; case K10/01). In the specimen with Ammon's horn sclerosis, NeuN-IR (C) reveals cell losses in the hilus and in sectors CA1 and CA3, whereas the subiculum (S) and the dentate granule cell layer are largely preserved. Dynorphin-IR (B) and GAD67-IR (A) mainly followed the pattern of the terminal field of mossy fibers (hilus of the dentate gyrus, stratum lucidum) and labeled the inner molecular layer (iml), which is aberrantly innervated by mossy fibers (mf). GAD67-IR was also present in the subiculum and extended (in contrast to dynorphin-IR) from the stratum lucidum (s. luc.) to the stratum pyramidale of sector CA1 (there labeling fibers of GABA neurons). VGAT-IR (E) and GAD65-IR (F) revealed an entirely different labeling pattern in adjacent sections of the same (sclerotic) specimen reflecting the distribution of fibers originating from GABA-ergic interneurons. In contrast to dynorphin-IR and GAD67-IR VGAT-IR (E) and GAD-65-IR (F) are faint in all terminal areas of mossy fibers, but label GABA-ergic fibers e.g. in the (inner and outer) molecular layer, in the stratum pyramidale CA1 and in the subiculum (E, F). Presumably due to neurodegeneration, the dentate hilus is weakly labeled for both markers (E, F). In D GAD67-IR is shown for a specimen without hippocampal sclerosis. It reveals a similar labeling pattern as the sclerotic specimen, except that the terminal area of sprouted mossy fibers in the inner dentate molecular layer lacks GAD67-IR. Presumably due to the lack of neurodegeneration, labeling of GABA neurons in the sector CA1 is also more prominent than in the sclerotic specimen. Arrowheads in A, B, D, E and F denote the borders between the stratum lucidum CA3 and stratum pyramidale CA2.

Scale bar: 1mm.

224x112mm (72 x 72 DPI)



38
39
40
41
42
43
44
45
46
47
48
49
50
51
52
53
54
55
56
57
58
59
60

FIGURE 3. Distribution of GAD67-IR, dynorphin-IR, and VGAT-IR in the molecular layer of the dentate gyrus of TLE patients with (A–C; patient E41) and without (D–F; patient E27) Ammon’s horn sclerosis. Dynorphin-IR serves as a specific marker for mossy fibers. VGAT labels the axons of GABA interneurons. In the specimen with Ammon’s horn sclerosis, the inner (iml) but not the outer molecular layer (oml) is intensely labeled for GAD67 (A) and dynorphin (B), whereas VGAT-IR labels the inner and the outer molecular layer equally. In the non-sclerotic specimen, labeling of the iml by GAD67 and dynorphin is absent (D, E). Dynorphin-IR in the middle and outer molecular layer (oml) presumably labels axon terminals of the perforant path (E). In the outer molecular layer, VGAT-IR axons of hilar GABA neurons terminate and can be well seen in the non-sclerotic specimen (F). Abbreviation: h, hilus, gc, granule cells. Scale bar: 100 μ m.

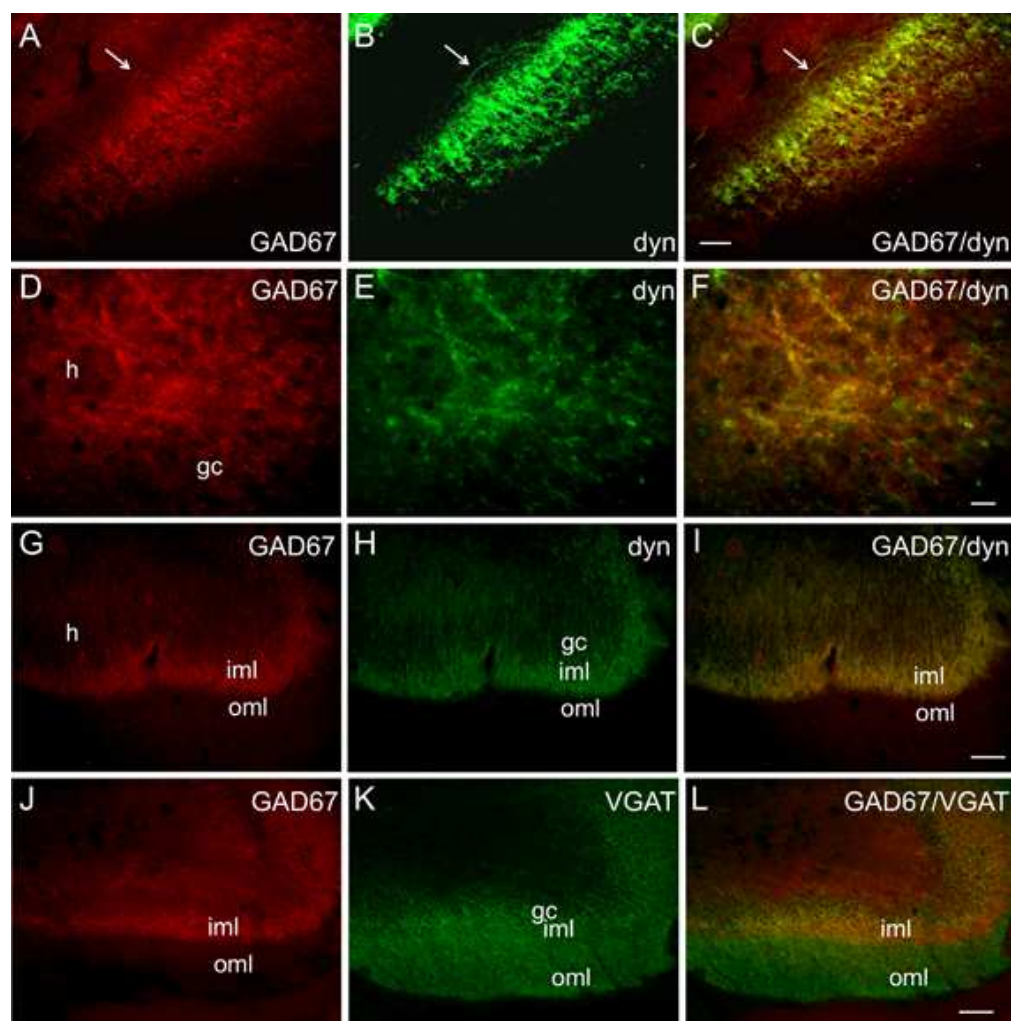


FIGURE 4. Double immunofluorescence for GAD67 and the mossy fiber marker dynorphin in terminal areas of mossy fibers (A–I) and of GAD67 and VGAT in GABAergic fibers of the dentate gyrus (J–L) in sections from patients with hippocampal sclerosis. A–C shows co-labeling of the stratum lucidum CA3 with GAD67- and dynorphin-IR (patient E18); D–F depicts co-labeling of mossy fiber bundles in the dentate hilus (h) with GAD67-IR and dynorphin-IR (patient E18). In G–I labeling of the dentate molecular layer of a sclerotic specimen is shown for GAD67- and dynorphin-IR (case 41). Note co-labeling of GAD67 with the mossy fiber marker dynorphin in the inner but not outer molecular layer (this is the terminal area of sprouted mossy fibers in hippocampal sclerosis). On the other hand, VGAT a marker of GABA-ergic neurons labels the outer molecular layer (K, L). Labeling for GAD67-IR again is strong in the inner (J, L) and faint in the outer (J) molecular layer. Scale bars: in C for A–C: 200 μ m; in F for D–F: 50 μ m, in I and L for G–L: 200 μ m.

200x202mm (72 x 72 DPI)

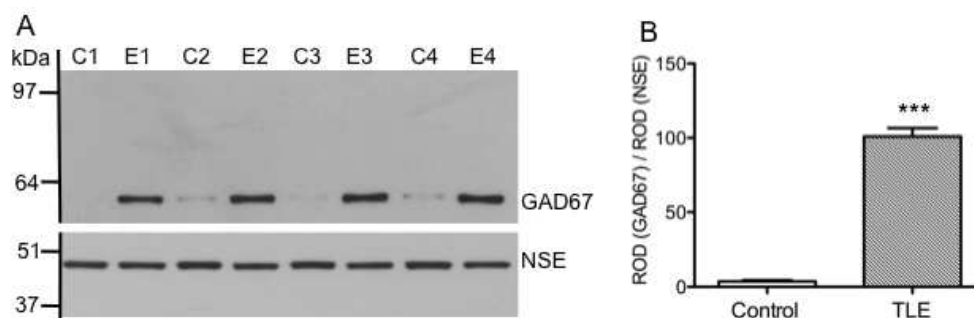


FIGURE 5. Immunoblots of dentate gyrus tissue from TLE patients. In A, a representative immunoblot of four arbitrarily selected, snap-frozen specimens from TLE patients (coded with E1 to E4) and post-mortem controls (C1 to C4) is shown. The blots were consecutively incubated with a monoclonal GAD67 antibody and an antibody for neuron-specific enolase (NSE). Single bands were observed for GAD67 both in control and in TLE tissue. Panel B depicts the ratios of ROD values obtained for GAD67 and NSE. ***Statistically different from controls ($p < 0.0001$) using the two-tailed Student's t-test.

222x73mm (72 x 72 DPI)

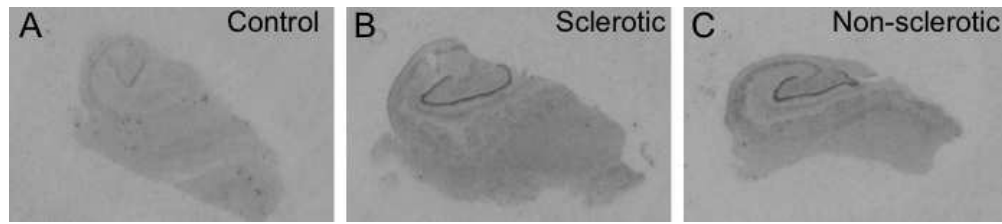


FIGURE 6. GAD67 mRNA. Autoradiographs of sections from the hippocampus of a post mortem control (A), a TLE specimen with (B, case 10/99) and one without hippocampal sclerosis (C, case G1/00). Note the pronounced up-regulation of GAD67 mRNA in dentate granule cells equally in the sclerotic and in the non-sclerotic specimen. Scale bar: 2 mm. For quantification see text.
244x52mm (72 x 72 DPI)

or Peer Review